CHAPTER 3

DNA-bound Redox Activity of DNA Repair Glycosylases Containing [4Fe4S] Clusters

Adapted from Boal, A. K., Yavin, E., Lukianova, O. A., O'Shea, V. L., David, S. S., and Barton, J. K. (2005) *Biochemistry 44*, 8397.

E. Yavin performed EPR experiments. O. Lukianova and V. O'Shea prepared protein samples.

INTRODUCTION

Encoded in the sequence of DNA is all of the genetic information of a cell. Yet the primary structure of DNA is remarkably dynamic (*1*). Large scale rearrangements lead to gross changes in sequence, while chemical modifications to individual bases may lead to single base mutations. The consequences of large- and small-scale DNA sequence alterations can be beneficial, allowing for increased genetic diversity, but more often are deleterious, leading to mutation and disease. To counteract the harmful nature of DNA modification, organisms have developed diverse repair machinery aimed at protecting the genetic code (*2*).

Damage to a single DNA base is commonly repaired by two different pathways: direct damage reversal that repairs a damaged base without excising it, and base excision repair (BER), a pathway that removes a single damaged base and replaces it with a new one (*3*). The first step in the BER pathway involves the glycosylase enzyme, a protein that locates the damaged base and excises it from the helix. The excision reaction catalyzed by glycosylases is relatively well understood at the molecular level, but the mechanism by which these enzymes locate their substrates in the first place remains elusive (*4*). This detection challenge faced by glycosylases is formidable on two fronts. First, the base mismatches and modifications, the substrates for the glycosylases, often occur at low frequencies and are isolated among a vast amount of undamaged DNA (*1*). Second, the damage products detected by these enzymes represent very subtle deviations from the four natural DNA bases; often they vary by the addition or subtraction of a single functional group or even simply the mismatching of otherwise natural base pairs.

Some evidence suggests that glycosylases locate damage by processing along the DNA helix rather than randomly diffusing from site to site (*5*). Processive mechanisms offer some enhancement in rate and efficiency by reducing the dimensionality of the search process. However, it is not clear that procession alone would be sufficient to account for the remarkable repair efficiency of these enzymes. In addition, BER enzymes operate in a complicated cellular environment, one in which a simple processive search process may be impossible (*6*). High salt concentrations exist that prevent electrostatic interactions between proteins and DNA (*7*). DNA is highly compact and covered in proteins much of the time, preventing rapid translocation along the helix (*8*). Glycosylases are often present in very low copy numbers (*9*) and may be involved in intricate relationships with other proteins, including those related to other repair pathways, replication, and transcription processes (*10-17*). All of these facts indicate that damage detection by glycosylases is a highly complex process, one that may require more than one mechanism.

The base pair π-stack of double helical DNA has the unique ability to serve as a medium for charge transport over distances of at least 200 Å (*18-23*). This property of DNA is highly dependent on the integrity of the π-stack; perturbations that affect the structure and dynamics of DNA, including mismatched base pairs and damage products, greatly diminish the efficiency of DNA charge transport (*24-27*). In fact, devices based on DNA-mediated charge transport have proven to be powerful sensors of mutation in DNA (*28*). Additionally, evidence suggests that DNA charge transport can occur in biologically relevant environments; within a nucleosome core particle (*29*) and inside the nucleus of HeLa cells (*30*). While a biological role for DNA-mediated charge transport has not been definitively established, it has been proposed that DNA charge transport

may be involved in DNA damage and repair (*31-33*). The exquisite sensitivity of DNA-mediated charge transport to perturbations in the π-stack prompts one to ask: might DNA repair enzymes exploit this property of DNA in their search for damage in the genome?

MutY, one of many glycosylases containing a [4Fe4S] cluster (*34-37*), has recently displayed redox activity when investigated electrochemically on DNA-modified electrodes (*33*). MutY, containing 350 residues and the [4Fe4S] cofactor, acts as a glycosylase to remove adenine from G:A and 7,8-dihydro-8-oxo-2-deoxyguanonsine (8-oxo-G):A mismatches (*38-52*). Initial characterization of the [4Fe4S] cluster in MutY and Endonuclease III (EndoIII), a homologous enzyme with a substrate specificity instead for damaged pyrimidines (*53-62*), demonstrated that the cluster is in the 2+ oxidation state and is not readily oxidized or reduced within a physiologically relevant range of potentials; cluster decomposition occurs with oxidation but photoreduction does yield the $[4Fe4S]^{1+}$ cluster (*34*). In the presence of DNA, however, MutY has a midpoint potential of +90 mV versus NHE (*33*). This redox potential is typical of high-potential iron proteins (*63*) indicating that, when MutY is bound to DNA, the redox potential of the enzyme shifts such that the 3+ oxidation state of the cluster becomes accessible. Earlier redox studies on MutY and EndoIII conducted in the absence of DNA had argued for a structural rather than redox role for the ubiquitous cluster (*52, 61-62, 64*), yet it was demonstrated that the [4Fe4S] cluster in MutY was not required for protein folding but was essential for activity (*65*).

Given the redox activity for MutY now demonstrated with DNA activation, a model has been proposed describing a role for the cluster in damage detection by MutY (*33*). In this model, DNA-mediated charge transport between two MutY proteins would serve as a fast, efficient scanning mechanism for damage in DNA; in the absence of intervening lesions, DNA charge transport between proteins would be facile, permitting

reduction with concomitant dissociation of the protein from undamaged regions of the genome. Through this fast scanning and sorting process, MutY would quickly concentrate near sites of damage in DNA. Local procession on a slower timescale to a nearby site would then allow for efficient substrate recognition and repair.

EndoIII and *A. fulgidus* UDG (AfUDG), like MutY, are glycosylases that contain a [4Fe4S] cluster (*34-35*). EndoIII repairs a wide variety of oxidized pyrimidines in DNA. The cluster in EndoIII is well characterized spectroscopically (*34, 64*). EndoIII is of particular significance because, as with MutY, it is present in many organisms (*66-68*). AfUDG, on the other hand, is part of a special class of uracil glycosylases (*69*). These enzymes, known as family 4 UDGs, are present mostly in thermophilic bacteria and are the only family of UDGs to contain a [4Fe4S] cluster (*35, 69-74*). Cytosine deamination, the main process by which uracil is produced in DNA, is greatly enhanced at high temperatures (*75*). In spite of this fact, thermophiles do not exhibit a higher mutation rate than other organisms (*76*). BER enzymes in thermophiles therefore face an even greater challenge to efficiently eliminate base damage. Perhaps the [4Fe4S] cofactor in these enzymes is involved in enhancing the efficacy of repair?

Here we determine whether the DNA-bound redox activity seen with MutY is a more general characteristic of DNA glycosylases containing a [4Fe4S] cluster. EndoIII and AfUDG are both investigated electrochemically on DNA-modified electrodes to determine if the [4Fe4S] cluster in each is redox-active and if that redox activity is DNA-mediated. Furthermore, all three proteins are examined by EPR spectroscopy with a Co(III) oxidant to establish whether DNA binding can also promote oxidation of the cluster in solution. These experiments have implications for the further development of our model to include the possibility of collaborative searching for damage by redox-active glycosylases.

MATERIALS AND METHODS

Materials

All buffers were freshly prepared and filtered prior to use. Potassium ferricyanide was purchased from EM Science. Poly(dGC) (ε_{260} = 8,400 $M^{-1}cm^{-1}$) was purchased from Amersham Pharmacia and was passed through spin columns (BioRad) prior to use. All reagents for DNA synthesis were purchased from Glen Research.

$[Co(phen)_3]Cl_3$ was synthesized from $CoSO_4.7H_2O$ according to a literature procedure (*77*). The cobalt complex was precipitated first as the PF_6 salt by adding a solution of NH_4PF_6 in water (20% w/v) to the reaction. The Co(III) complex was then converted to its chloride salt by dissolving 200 mg $[Co(phen)_3]PF_6$ in 5 ml CH_3CN followed by the addition of $(tBu)_4NCl$ in 3 mL CH_3CN (20% w/v) and formation of a yellow precipitate. After filtration and washing with acetonitrile, the isolated complex $[Co(phen)_3]Cl_3$ was fully characterized by NMR and mass spectrometry.

Protein Preparation

EndoIII was generously donated by Professor T. R. O'Connor (City of Hope) (*78*). The purification of AfUDG was modified from the reported procedure (*74*). The pET28a-*afung* plasmid containing the gene encoding the AfUDG protein was provided by Dr. William A. Franklin (Albert Einstein). Rosetta(DE3)pLysS cells (Novagen) transformed with the pET28a-*afudg* plasmid were inoculated into LB media containing 34 μg/mL kanamycin and grown at 37 °C in 4L to an OD_{600} = 0.5-0.7. At this stage, 1 mM isopropyl-1-thio-β-D-galactopyranoside (IPTG) was added, and the cells were incubated

for an additional 6 hours at 30 °C. The cells were harvested by centrifugation (10000 rpm, 7 minutes, 4 °C), resuspended in 40 mL of ice-cold buffer L (25 mM Tris, 250 mM NaCl, pH 7.6) supplemented with 1 mM PMSF. The cells were disrupted by sonication (Branson Sonic Power CO., model 350, 70% pulse, 30 s on followed by 30 s off, repeated six times), and centrifuged to remove cellular debris (10000 rpm, 5 minutes, 4 °C). The proteins in the supernatant were batch-bound to Ni^{2+}-NTA resin (1.5 mL/40 mL supernatant) by gentle rocking at 4 °C for 1 hour. The protein-bound resin was poured into an empty column (10 mL) and washed with 25 mL of 2X buffer L, followed by 5 mL of 1X buffer L. Protein was eluted with 2-5 mL of 1X buffer L containing 250 mM imidazole and diluted 8-10 fold with Buffer A (25 mM Tris, pH 7.6). The protein solution was loaded onto a High S cartridge (BioRad), pre-equilibrated with 90% Buffer A and 10% Buffer B (25 mM Tris, pH 7.6, 1 M NaCl). The AfUDG protein was eluted by increasing the concentration of buffer B. Glycerol (10%) was added to the protein solution for storage at -80 °C. SDS-PAGE with Sypro Orange staining indicated the protein to be greater than 95% pure. Total protein concentrations were determined by the method of Bradford using BSA as the standard.

MutY was utilized fused to maltose binding protein to allow experiments to be carried out at high concentrations. JM101 *mutY- E. coli* cells containing a pMAL-c2x-*muty* vector encoding maltose binding protein fused to the N-terminus of MutY were used to inoculate LB media (200 mL) containing 100 μg/mL ampicillin, 15 μg/mL tetracycline, and 0.2 g/mL glucose (LBATG). After overnight incubation at 37 °C, the culture was added to 4 L LBATG which was further incubated with shaking at 37 °C until the OD at A_{600} was 0.6. IPTG (0.3 mM) was then added and the cells were incubated at 30 °C for 3.5 hours. After centrifugation (10,000 rpm for 7 minutes), the cells were

resuspended in 30 mL of 50 mM Tris-HCl pH 8 containing 2 mM EDTA, 5% glycerol, 250 mM NaCl, 5 mM DTT, and 1 mM PMSF. The cells were lysed using a French press, the process being repeated twice, followed by centrifugation to remove cellular debris. The cell lysate (~ 40 mL) was loaded onto two separate 20 mL amylose (New England BioLabs) columns pre-equilibrated with Buffer C (20 mM HEPES-KOH pH 7.5 at 4 °C, 200 mM NaCl, 1 mM EDTA, and 1 mM DTT). MutY was eluted using 50 mL buffer C containing 10 mM maltose. The protein-containing eluent was diluted twofold with buffer D (20 mM HEPES-KOH pH 7.5 at 4 °C, 1 mM EDTA, 5% glycerol, and 1 mM DTT), filtered with a 0.45 micron filter, and loaded onto a 5 mL heparin column (Amersham Biosciences) on a BioRad BioLogic. MutY was eluted using a gradient of 5 – 100% buffer D containing 1 M NaCl. Fractions containing pure MutY, as determined by SDS-PAGE with Sypro-orange staining, were concentrated and the buffer exchanged (20 mM Na-Phosphate pH 7.5, 100 mM NaCl, 10% glycerol, 1 mM EDTA) using an Amicon stirred ultrafiltration cell. The protein concentration was determined using an approximate ε(410 nm) of 17,000 $M^{-1}cm^{-1}$.

Preparation of DNA-modified Electrodes

Oligonucleotides were synthesized using standard phosphoramidite chemistry (*79*). Single strand oligonucleotides were modified at the 5' end with a thiol moiety to facilitate covalent attachment to a gold electrode surface, as described earlier (*80*). Oligonucleotides were purified by HPLC, hybridized to their complements and self-assembled into a loosely packed monolayer on a Au surface (*27*) in 50 mM NaCl, 5 mM sodium phosphate, pH 7.0. The electrode surface was then further passivated by incubation using mercaptohexanol (100 mM) in assembly buffer for 30 minutes.

Electrodes were then rinsed with protein storage buffer (MutY and EndoIII: 100 mM NaCl, 20 mM sodium phosphate, 1 mM EDTA, 10% glycerol, pH 7.0; AfUDG; 25 mM Tris-HCl, 500 mM NaCl, 5% glycerol, pH 7.6), and 50 μL protein (550 μM MutY, 150 μM EndoIII, or 360 μM AfUDG) in their storage buffers were added to the electrode surface and allowed to incubate for 10–15 minutes prior to measurement.

Electrochemistry Measurements

Low volume constraints necessitated the use of a specialized low-volume cell for protein electrochemistry experiments. The working electrode consisted of a Au(111) on mica chip and a Pt wire served as the auxiliary electrode. The reference electrode was a Ag/AgCl electrode modified with a tip containing 4% agarose in 3 M NaCl. This reference electrode was calibrated with ferrocene carboxylate and compared both to an unmodified Ag/AgCl reference electrode and a saturated calomel electrode. All measurements were made using a BAS CV50W model electrochemical analyzer.

EPR Spectroscopy

X-band EPR spectra were obtained on a Bruker EMX spectrometer equipped with a rectangular cavity working in the TE_{102} mode. Low temperature measurements (10K) were conducted with an Oxford continuous-flow helium cryostat (temperature range 3.6–300 K). A frequency counter built into the microwave bridge provided accurate frequency values. Solutions were prepared by adding the protein (50 μM) to a solution of oxidant (150 μM) (with the exception of EndoIII where the protein concentration was 10 μM and the oxidant concentration was 30 μM) in the presence or absence of poly(dGC) (1.5 mM in base pairs). Samples were incubated at ambient

temperature (10 min) or heated to 55 ºC (5 min) and cooled down to ambient temperature. All samples were frozen in liquid nitrogen prior to EPR measurement at low temperature. EPR parameters were as follows: receiver gain = 5.64×10^3, modulation amplitude = 4G, microwave power = 1.27 mW.

RESULTS AND DISCUSSION

Electrochemistry on DNA-modified Electrodes

The redox properties of each protein (MutY, EndoIII, and AfUDG) were investigated on a loosely packed DNA-modified electrode surface passivated with mercaptohexanol (MCH) (Figure 3.1). AfUDG and EndoIII both exhibit a redox signal using a DNA-modified electrode (Figure 3.2). The midpoint potential for AfUDG is 95 ± 3 mV versus NHE, while the midpoint potential for EndoIII is 58 ± 6 mV versus NHE. The measured midpoint potentials are similar to that previously measured for MutY of 90 mV versus NHE (*33*). The signals observed are quasi-reversible and robust over the course of the experiment. For each protein, the signal grows in over 5-10 minutes and remains at a constant intensity for up to 30 minutes after addition of the protein. No evidence of cluster degradation is observed during the experiment. Scan rate dependence measurements show a linear relationship between the peak current and the square root of the scan rate, an indication of a diffusion-limited process. However, measurements of electron transfer rates based on peak splitting (*81*) indicate a relatively slow rate of electron transfer (1–10 s^{-1}), consistent with earlier measurements of MutY (*33*). Importantly, as shown in Figure 3.2, each protein requires DNA for redox activity; at a MCH-modified surface lacking DNA, no signal is evident. In fact, even with 1 mM protein, no redox signal could be observed.

Figure 3.1. Schematic illustration of the electrochemical measurement of DNA-binding proteins containing [4Fe4S] clusters at a DNA-modified Au electrode surface.

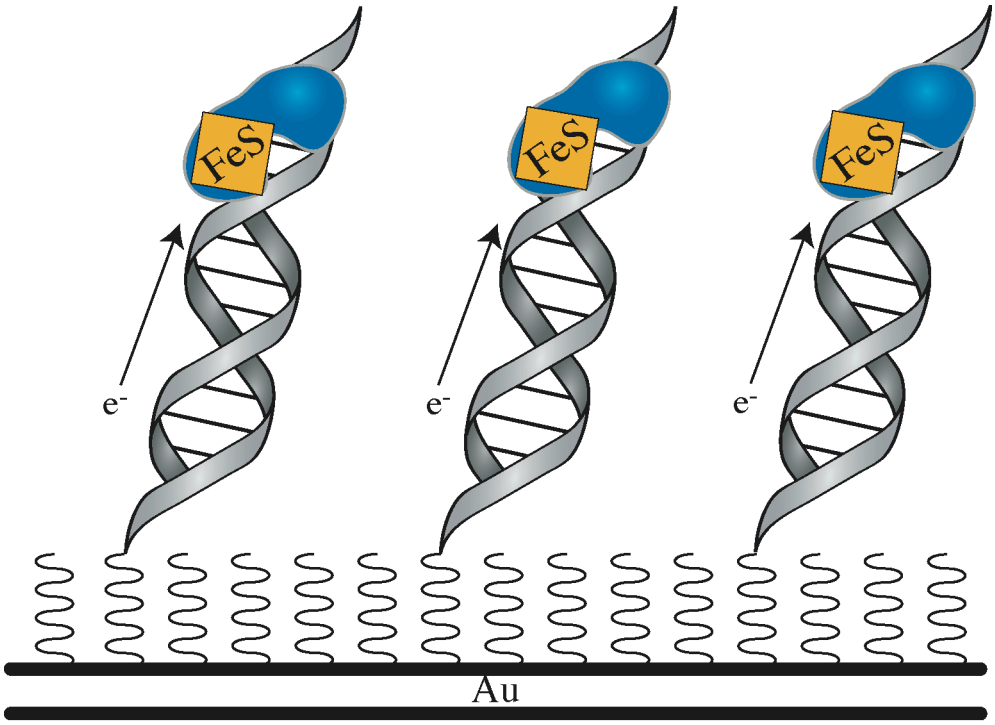

Figure 3.2. Cyclic voltammetry of MutY (left), EndoIII (middle), and AfUDG (right) at DNA-modified electrodes (shown in black) (Ag/AgCl reference electrode, Pt auxiliary electrode, 50 mV/sec scan rate). Buffer conditions for MutY and EndoIII are 100 mM NaCl, 20 mM sodium phosphate, 1 mM EDTA, 10% glycerol, pH 7.0. Buffer conditions for AfUDG are 25 mM Tris-HCl, 500 mM NaCl, 5% glycerol, pH 7.6. Average potentials, based on several trials, are 90 mV for MutY, 59 mV for EndoIII, and 95 mV for AfUDG, all versus NHE. DNA is required to observe the protein redox activity; proteins examined on a MCH-modified electrode (shown in grey) exhibit no electrochemical signal.

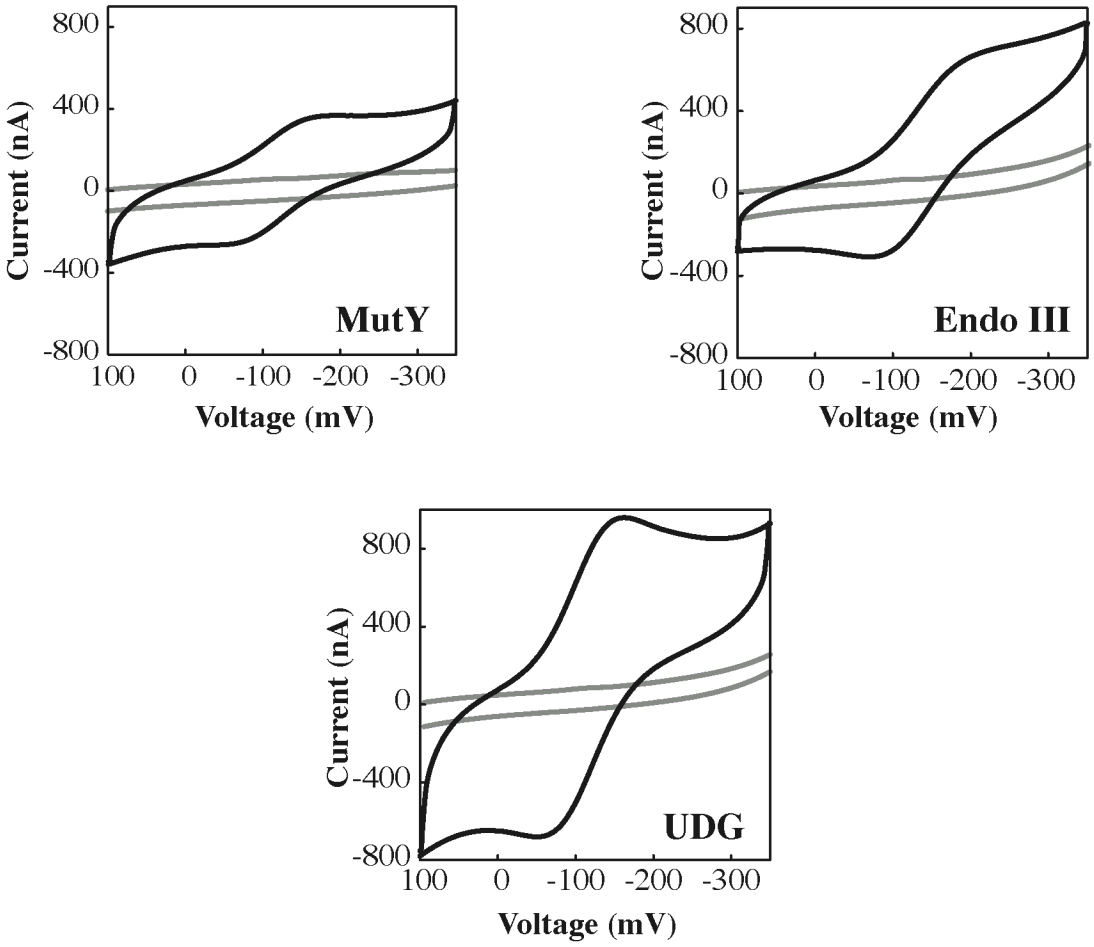

Covalent modification of electrodes is a technique commonly employed in protein electrochemistry both to concentrate proteins at the electrode surface and to properly orient buried redox centers for direct electron transfer with the electrode (*82-83*). To determine whether the redox activity observed here at a DNA-modified electrode is the result of direct interaction between the protein and the electrode surface or whether electron transfer to the cluster is mediated by the DNA π-stack, these proteins were investigated at a surface modified with a duplex containing an abasic site (thiol modified strand SH-5'-AGTACAGTCATCGCG hybridized to a complement containing an abasic site opposite the underlined thymine). We have determined previously that an intervening abasic site serves to diminish the redox signal from DNA-bound probes owing to the associated perturbation to the base pair stack (*28*). As evident in Figure 3.3, when each of these proteins is monitored electrochemically on a monolayer containing an abasic site, the redox signal is significantly attenuated. These observations support the idea that the redox chemistry obtained is DNA-mediated. The potential determined is therefore characteristic of the *DNA-bound* protein.

To test further that DNA binding promotes the shift in +3/+2 redox potential, activating the protein towards oxidation, we examined the protein electrochemistry on the DNA-modified surface before and after bulk electrolysis. Shown in Figure 3.4 are cyclic voltammograms for EndoIII bound to the DNA-modified electrode before and after shifts in applied potential. As is evident, when the sample is equilibrated and then the potential is held at –350 mV for a discrete time interval so as to reduce the DNA-bound protein, the signal is attenuated, consistent with reduced protein dissociating from the DNA-modified electrode. Similarly, as is also shown in Figure 3.4, when the potential is held at +50 mV, to promote oxidation, the signal increases, consistent with protein

Figure 3.3. Electrochemistry (clockwise from top right) of MutY, AfUDG, and EndoIII at an electrode modified with well matched DNA duplexes (TA DNA in black) or DNA duplexes containing an abasic site (Ab DNA in grey) as measured by cyclic voltammetry (Ag/AgCl reference electrode, Pt auxiliary electrode, 50 mV/sec scan rate). Buffer conditions for MutY and EndoIII are 100 mM NaCl, 20 mM sodium phosphate, 1 mM EDTA, 10% glycerol, pH 7.0. Buffer conditions for AfUDG are 25 mM Tris-HCl, 500 mM NaCl, 5% glycerol, pH 7.6.

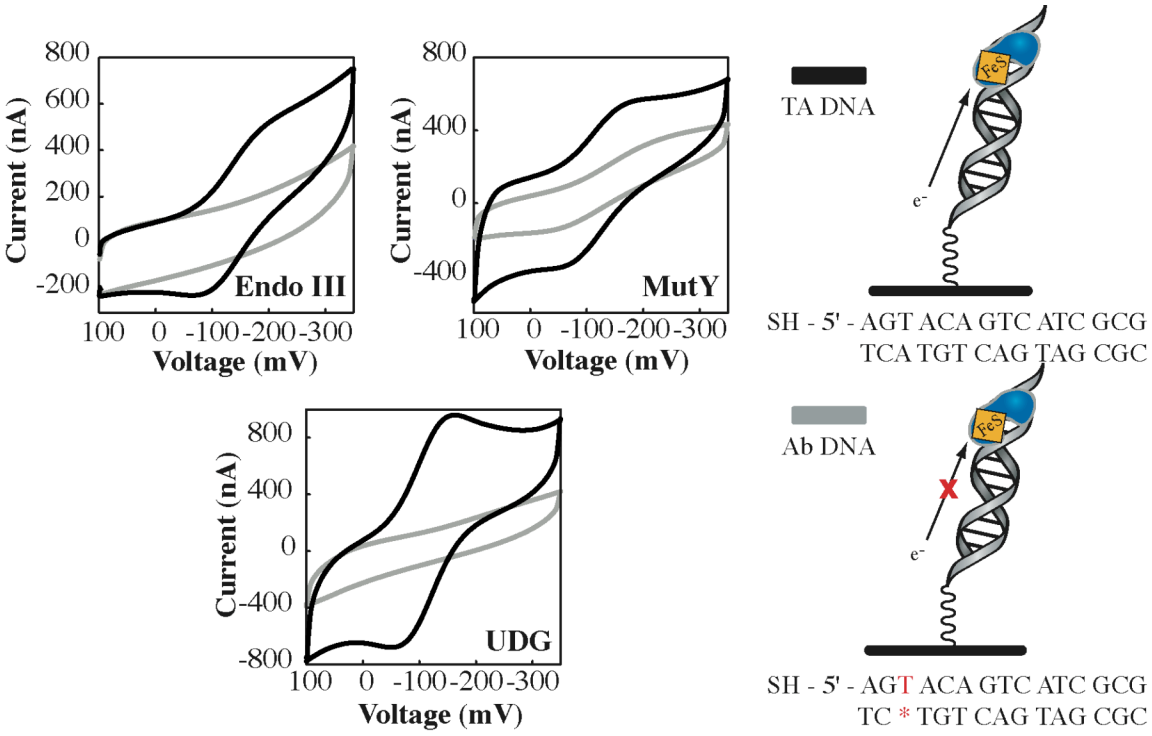

Figure 3.4. Cyclic voltammetry of EndoIII before and after bulk electrolysis. Left panel shows CV before (grey trace) and after (black trace) bulk electrolysis for 5 minutes at -350 mV (versus Ag/AgCl). Right panel shows CV before (grey trace) and after (black trace) bulk electrolysis for 5 minutes at +50 mV (versus Ag/AgCl). An increase in peak intensity is evident after electrolysis at +50 mV, whereas a corresponding decrease is observed after electrolysis at -350 mV.

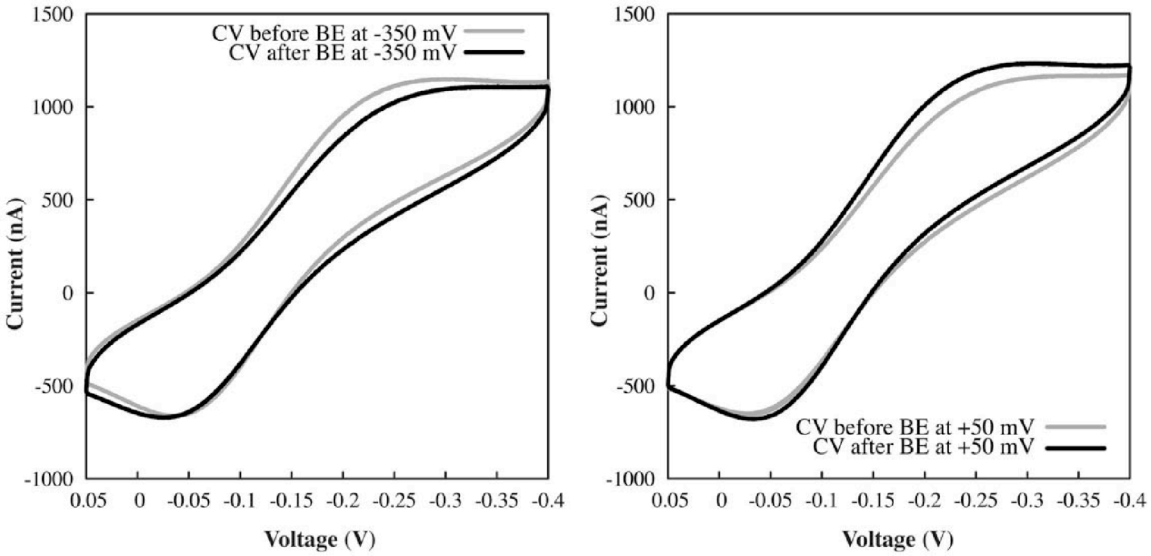

oxidation yielding association with DNA. Calculation of net changes in area under the cyclic voltammograms reveal a 14% difference in both directions as a result of electrolysis. Analogous results were found with the other BER enzymes examined. While these results cannot provide a quantitative determination of solution binding affinities, these data nonetheless provide support for a greater DNA affinity for the protein in the oxidized form versus the reduced +2 state.

Low Temperature EPR to Probe DNA-bound Redox Chemistry

All three proteins were investigated by EPR spectroscopy in the presence and absence of DNA using $Co(phen)_3^{3+}$ as the oxidant. EPR measurements were performed at 10K to observe any changes in the oxidation state of the [4Fe4S] cluster. The [4Fe4S] cluster in each of these proteins is in the 2+ oxidation state when free in solution, a configuration that is diamagnetic and EPR-silent (*34-35, 84*). However both the $[4Fe4S]^{3+}$ and $[3Fe4S]^{1+}$, a common damage product resulting from hydrolysis of the oxidized [4Fe4S] cluster (*63, 85-86*), are EPR-active and give rise to distinctive spectra (*84, 87-90*).

As expected, MutY, in the presence and absence of DNA, yields no EPR signal. The $[4Fe4S]^{2+}$ cluster in MutY is largely in the 2+ oxidation state and EPR-silent. When MutY (50 μM) is incubated with $[Co(phen)_3]^{3+}$ (150 μM), a small signal appears, that looks much like a [3Fe4S] cluster (*85, 89-90*) with g values at 2.02 and 1.99 (Figure 5). In the presence of DNA and $[Co(phen)_3]^{3+}$ (150 μM), this signal is also evident but the intensity is much greater (~ 4-fold by integration). It appears then that the presence of DNA enhances oxidation by Co(III). Since the cobalt complex binds DNA (*91-92*), albeit weakly, we also examined the oxidation reaction with an excess of $[Co(phen)_3]^{3+}$.

Figure 3.5. EPR spectroscopy at 10K of MutY in the presence of DNA (light grey), 150 μM $[Co(phen)_3]^{3+}$ without DNA (dark grey), 500 μM $[Co(phen)_3]^{3+}$ but no DNA (dotted line), and MutY with DNA and 150 μM Co(III) (black). Signal 1 shows g = 2.02, signal 2 shows g = 1.99.

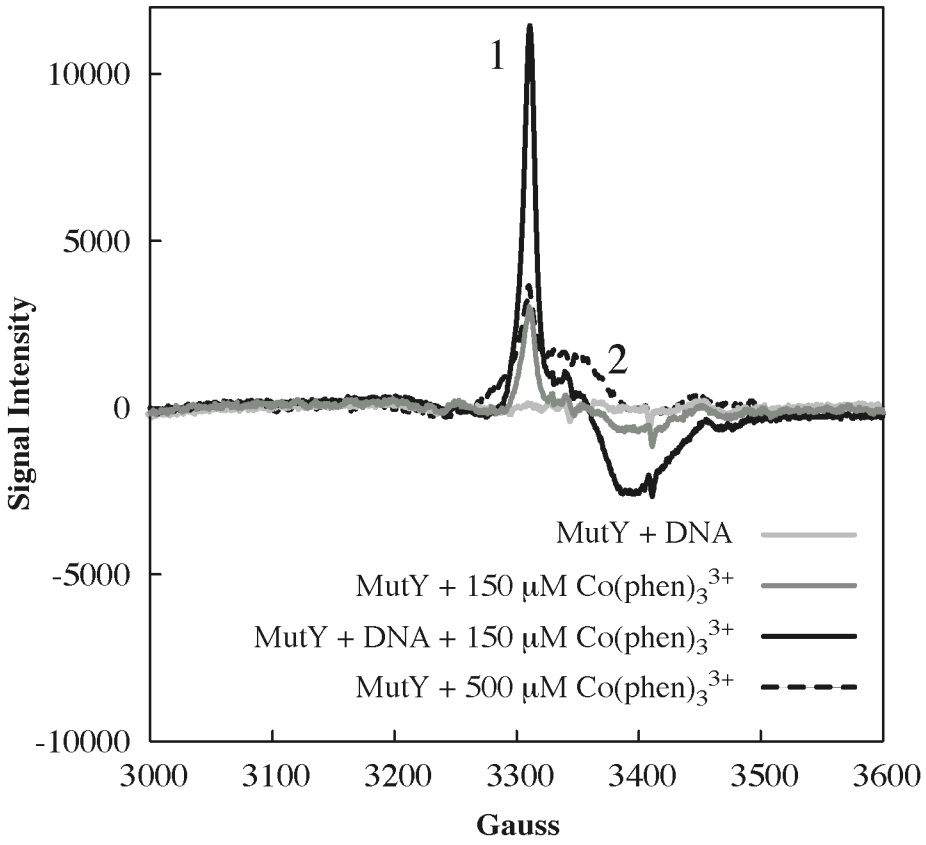

Addition of 500 μM $[Co(phen)_3]^{3+}$ in the absence of DNA results in a small increase in signal intensity; some interaction of the protein with the cobalt complex at these high concentrations is expected, yet without DNA little reaction occurs. These results are therefore consistent with DNA binding serving to shift the oxidation potential of the cluster, activating the cluster towards oxidation.

EndoIII also does not exhibit an EPR signal without oxidant in the presence or absence of DNA. Like MutY, upon addition of $[Co(phen)_3]^{3+}$ (30 μM) to EndoIII (10 μM), a signal appears with g = 2.03 and 2.01, consistent with formation of a $[3Fe4S]^{1+}$ cluster (Figure 3.6) (*89-90*). This signal also increases in intensity in the presence of DNA, although the enhancement is not as high as for MutY.

We also examined repair protein oxidation by ferricyanide in the presence and absence of DNA. A similar enhancement in cluster oxidation was observed in the presence of DNA (data not shown). However, ferricyanide is also known to promote oxidation of the cluster without DNA (*34-35*).

AfUDG in the presence or absence of DNA is EPR-silent as well. Unlike MutY and EndoIII, AfUDG (50 μM) in the presence of $[Co(phen)_3]^{3+}$ (150 μM) is also EPR silent in the absence of DNA. When DNA is included, however, a signal appears with g values at 2.13 and 2.04, typical of a $[4Fe4S]^{3+}$ cluster (*87-88*) (Figure 3.7). Since AfUDG is isolated from a thermophilic organism, these samples were also investigated following incubation at 55 ºC for five minutes. The same pattern is evident; AfUDG with DNA is EPR silent, as is AfUDG with $[Co(phen)_3]^{3+}$, while AfUDG with DNA and $[Co(phen)_3]^{3+}$ elicits a signal. However this signal has a g value of 2.02, indicating that the cluster is likely in the $[3Fe4S]^{1+}$ configuration. Previous studies examining oxidation

Figure 3.6. EPR spectroscopy at 10K of EndoIII in the presence of DNA (light grey), 150 μM $[Co(phen)_3]^{3+}$ without DNA (dark grey), and with both DNA and 150 μM Co(III) (black). Signal 1 shows g = 2.03, signal 2 shows g = 2.01.

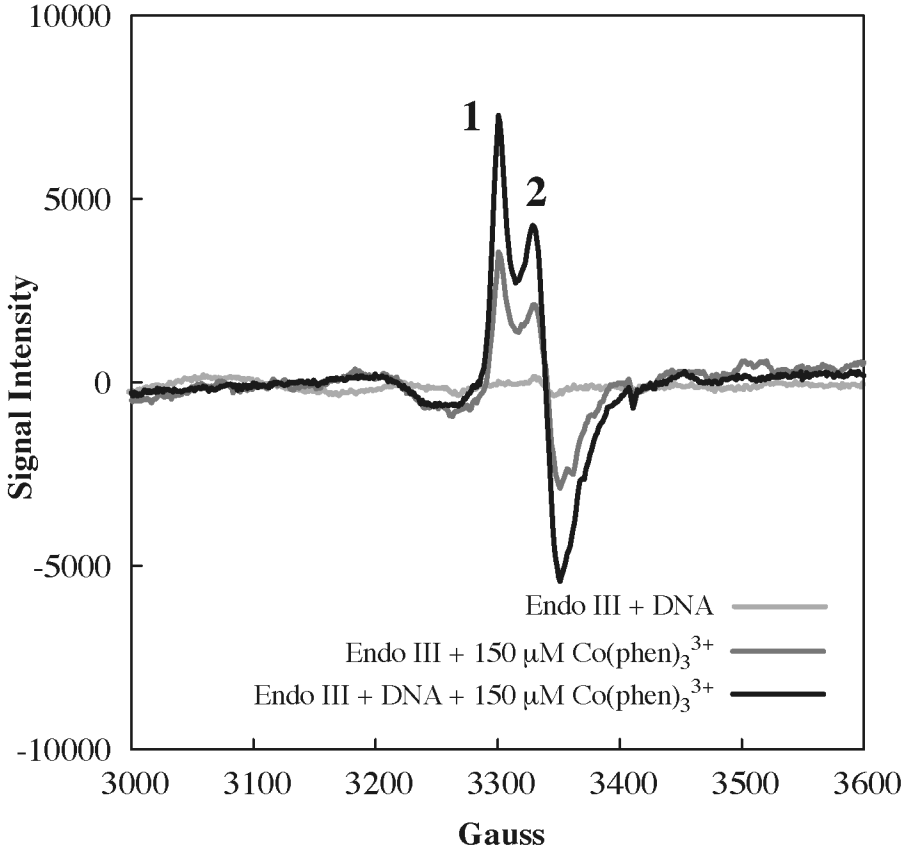

Figure 3.7. EPR spectroscopy at 10K in AfUDG in the presence of DNA (light grey), 150 μM $[Co(phen)_3]^{3+}$ without DNA (dark grey), and with both DNA and 150 μM Co(III) (black). Shown above after incubation at ambient temperature and below after incubation at 55 ºC. Signal 1 shows g = 2.13; signal 2 shows g = 2.04; signal 3 shows g = 2.02.

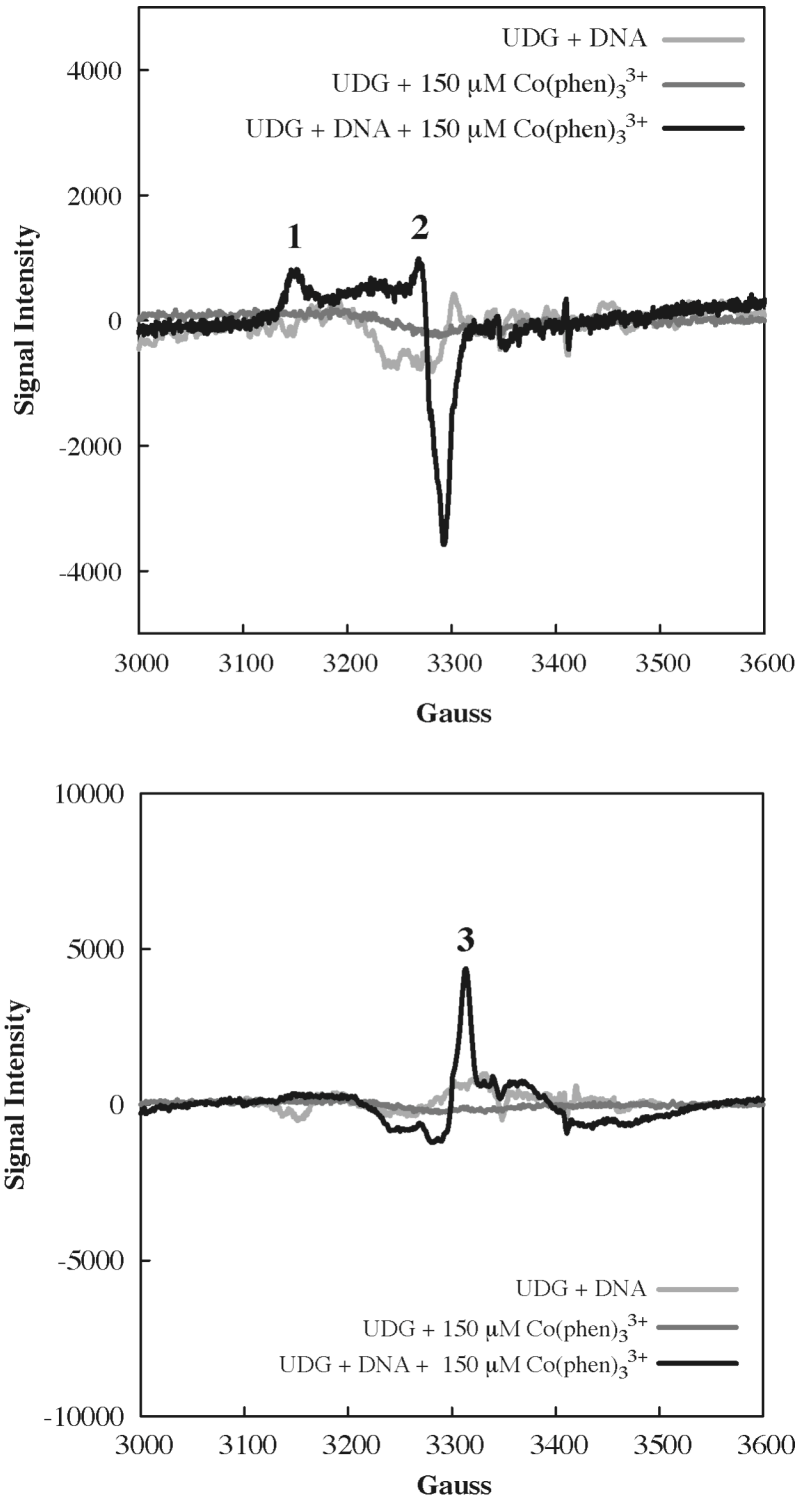

of the cluster in family 4 UDG from *Pyrobaculum aerophilum* by ferricyanide demonstrated that a mixture of $[4Fe4S]^{3+}$ and $[3Fe4S]^{1+}$ species are formed in the absence of DNA (*35*). It is therefore apparent that this repair enzyme also is activated toward oxidation of its [4Fe4S] cluster upon DNA binding.

Redox Activation of BER Enzymes upon DNA Binding

Electrochemical measurements of EndoIII and AfUDG using DNA-modified electrodes demonstrate that, like MutY, both of these enzymes that contain a [4Fe4S] cluster are redox-active when bound to DNA. Both BER enzymes have physiologically relevant redox properties when evaluated on DNA-modified electrodes, with potentials of ~ 100 mV versus NHE, typical of high-potential iron proteins (*63*), and similar to MutY (*33*). Solution studies with mediators have shown that the proteins could not be easily oxidized in the absence of DNA, and the more accessible 2+/1+ couple was estimated to be < -600 mV versus NHE (*34*). Without DNA attached to the gold electrodes, neither oxidation nor reduction of these proteins is observed electrochemically. Thus protein binding to DNA appears to shift the redox potential, activating the $[4Fe4S]^{2+}$ cluster towards oxidation.

Further support for this redox activation is apparent in monitoring changes in DNA-bound protein as a function of applied potential. When the DNA-modified electrodes are equilibrated with protein, but then the applied potential is shifted towards more negative potentials, reducing the protein, some protein dissociation from the electrode is evident. Similarly, shifting the potential to more positive values, to promote oxidation, increases the DNA-bound protein signal. While these data do not provide a quantitative measure of the difference in DNA binding affinity with protein in the reduced versus oxidized form, these data do qualitatively support an increase in binding affinity

for the protein with the [4Fe4S] cluster in the +3 state versus the +2 state. In other words, thermodynamically, DNA binding activates the protein towards oxidation. A quantitative determination of this difference in binding affinity for the protein with cluster in the +3 versus +2 form may not be possible technically, since cluster oxidation in the absence of DNA clearly leads to cluster decomposition. On the DNA-modified electrodes, however, the redox cycle appears to be reversible.

That DNA binding would shift the potential is reasonable to expect. The redox potentials of $[4Fe4S]^{2+}$ clusters are well known to vary considerably depending upon their environment (*63, 93*). Based on crystal structures of MutY (*94*) and EndoIII (*95*) bound to DNA, it is apparent that the iron-sulfur cluster is located near amino acid residues that contact DNA, so that DNA binding changes the environment for the cluster, taking it from an exposed and polar environment in the absence of DNA to a more hydrophobic environment in the presence of DNA. Moreover, the substrate binding affinity of MutY has been shown to be extremely sensitive to alterations of amino acids in the cluster coordination domain consistent with an intimate association of this region with DNA (*84*). It is reasonable to consider, then, that in the absence of DNA, the [4Fe4S] cluster is more ferredoxin-like, with the 2+/1+ couple being more accessible (*96*). Estimates for the reduction potential for the $[4Fe4S]^{2+}$ cluster of EndoIII of ~ -600 mV are consistent with this characterization. However, DNA binding may make the cluster environment more similar to high potential iron proteins, with the 2+/3+ couple being more accessible in the physiological regime (*96*). Indeed, the DNA-bound potentials of 100 mV we observe are characteristic of high potential iron proteins. Estimates based upon model studies for the difference in potential for the 3+/2+ couple versus the 2+/1+ couple are $\geq$ 1.0 V, both for ferredoxin-like clusters and high potential iron centers (*63,*

93, 96). Using a conservative value of 1.0 V for this difference, a value of –600 mV for the 2+/1+ cluster potential of EndoIII without DNA, and the measured potential of 90 mV for the DNA-bound 3+/2+ couple, suggests that DNA binding shifts the 3+/2+ potential 310 mV more negative. Thermodynamically this 300 mV shift would correspond to a change in binding affinity between the 2+ and 3+ states of more than 4 orders of magnitude.

The EPR results also are consistent with DNA binding activating the cluster towards oxidation. While some oxidation by $Co(phen)_3^{3+}$ in the absence of DNA is found, significant enhancements in oxidation are apparent in the presence of DNA. Earlier results had shown some evidence of irreversible oxidation of EndoIII by ferricyanide (*34*), but no enhancement with DNA binding was explored. Here it is noteworthy that $Co(phen)_3^{3+}$, an oxidant with potential similar to ferricyanide, binds to DNA (*91-92*). Hence the enhancement could reflect an increase in local concentration of the cobalt complex near the DNA-bound BER enzyme; ten times higher concentrations of $Co(phen)_3^{3+}$ without DNA showed no increased oxidation, however. Alternatively, the oxidation of the protein by $Co(phen)_3^{3+}$ might be DNA-mediated. $Co(phen)_3^{3+}$ binds DNA by partial intercalation (*92*), facilitating coupling into the base pair stack to enable a DNA-mediated reaction.

The electrochemical results using DNA-modified electrodes show clearly that the charge transport reaction to oxidize the cluster can be DNA-mediated. With all of these proteins, incubation at a DNA-modified surface containing an abasic site yields a drastically attenuated signal compared to that found with a well matched DNA duplex. This attenuation indicates that the DNA base pair stack must mediate electron transfer to the cluster, rather than simply serving to locally concentrate the enzyme at the electrode. DNA-mediated charge transfer to the cluster requires an intact base-pair π-stack.

Characteristics of the Oxidized Protein

EPR spectroscopy is used commonly to characterize [4Fe4S] clusters and their oxidation states. Based upon comparative g values, MutY, EndoIII, and AfUDG, upon DNA binding in the presence of an oxidant, primarily promote formation of the $[3Fe4S]^{1+}$ cluster. Some evidence for the $[4Fe4S]^{3+}$ cluster is also found, however, with AfUDG upon DNA binding.

High-potential iron proteins are known to be susceptible to degradation through reaction with water and oxygen (*63*);

$$[4Fe4S]^{2+} \xrightarrow[ox.]{DNA} [4Fe4S]^{3+} \quad (1)$$

$$[4Fe4S]^{3+} \xrightarrow[O_2]{H_2O} [3Fe4S]^{1+} \quad (2)$$

the $[4Fe4S]^{3+}$ cluster can lose an iron to form the $[3Fe4S]^{1+}$ cluster. This degradative process frequently occurs in [4Fe4S] proteins as a result of oxidative damage (*85*). While the electrochemistry results indicate that DNA activates the $[4Fe4S]^{2+}$ cluster towards oxidation in all three proteins and that oxidation can be reversed, MutY and EndoIII only show a signal typical of a $[3Fe4S]^{1+}$ cluster by EPR spectroscopy. With MutY and EndoIII, it is likely that the low temperature required to observe the cluster by EPR (10K) destabilizes the protein such that the cluster falls apart; electrochemistry results are obtained instead at ambient temperatures in buffer. Since this degradation process first requires oxidation of the $[4Fe4S]^{2+}$ cluster to the $[4Fe4S]^{3+}$ state (eq. 1, 2), the $[3Fe4S]^{1+}$ signal indicates, indirectly, oxidation of the cluster.

EPR experiments with AfUDG, furthermore, do show signals characteristic of a $[4Fe4S]^{3+}$ cluster in solution when the protein is incubated with DNA and $[Co(phen)_3]^{3+}$. Interestingly, when this same sample is first heated to 55 ºC, the degraded cluster ($[3Fe4S]^{1+}$) is observed instead. Oxidation of AfUDG with ferricyanide earlier had shown EPR evidence of both the $[4Fe4S]^{3+}$ and $[3Fe4S]^{1+}$ clusters (*35*), and here with DNA binding and oxidation with cobalt, a species with g values of 2.13 and 2.04, generally characteristic of a $[4Fe4S]^{3+}$ cluster (*83-84*), is observed. Noteworthy also are fluorescence studies of AfUDG as a function of temperature (*71*) which suggested that, above 50 ºC, AfUDG has a more "open" conformation, while the structure is more compact at lower temperature; this also was correlated with the higher activity of the enzyme above 50 ºC. It seems that this more "open" conformation is more susceptible to hydrolytic degradation of the $[4Fe4S]^{3+}$ cluster, leading to formation of the $[3Fe\text{-}4S]^{1+}$ cluster (based on the appearance of a species with a g-value of 2.01).

It is interesting in this context to consider recent results we have obtained for the DNA-mediated oxidation of MutY by guanine radical (*97*). Oxidized guanine radical in DNA, generated using a flash/quench technique, is found to promote oxidation of the $[4Fe4S]^{2+}$ cluster of MutY primarily to $[4Fe4S]^{3+}$ along with its decomposition product $[3Fe4S]^{1+}$ based upon EPR spectra with g values of 2.08, 2.06, and 2.02. Thus oxidation of the cluster in a rapid DNA-mediated reaction is far more likely to yield $[4Fe4S]^{3+}$ with minimum decomposition.

Model for Collaborative Scanning for DNA Lesions by BER Enzymes

While the enzymology of BER enzymes has been increasingly well established, little is understood about how BER repair enzymes first locate their substrates, often

single damaged bases in a vast array of undamaged DNA (*1*). The [4Fe4S] clusters are ubiquitous to these enzymes although a redox function for these clusters had been disregarded owing to the lack of redox activity seen with these proteins under physiological conditions (*34*). The data reported here, where DNA binding promotes a shift in redox potential to the physiological range, for all three BER enzymes, now requires that a redox role for these [4Fe4S] clusters be revisited.

We propose that the clusters serve as cofactors for DNA-mediated redox signaling among the BER enzymes. Through long range DNA-mediated charge transport, the BER enzymes may quickly become localized in regions of the genome containing DNA mismatches and lesions. This model is based upon the shift in potential we find for the BER enzymes associated with DNA binding. Thus our proposal reflects the electron exchange reaction among BER enzymes of similar potential bound to DNA so that

$$[4Fe4S]_A^{2+} + \{DNA\text{-}[4Fe4S]_B^{3+}\} \rightleftharpoons \{DNA\text{-}[4Fe4S]_A^{3+}\} + [4Fe4S]_B^{2+} \quad . \qquad (3)$$

Figure 3.8 illustrates this model for this cooperative BER detection strategy. A given BER enzyme, free in solution, contains the [4Fe4S] cluster in the 2+ state, as seen earlier (*34-35, 84*). As such, the protein is robust and insensitive to redox chemistry. As shown here, binding to DNA, however, shifts the redox potential, facilitating oxidation of the [4Fe4S] cluster to the +3 state. Oxidation, then, can involve a DNA-mediated charge transfer to an alternate BER enzyme bound at a distal site along the DNA with its cluster already in the +3 state. Reduction of this secondary BER enzyme could then facilitate its dissociation from the duplex. This process, as described, in actuality represents a scan

of one region of the genome: in the absence of an intervening lesion, mismatch, or other perturbation in base pair stacking, the DNA-mediated charge transfer process can proceed. The similarity in potentials for the different DNA-bound BER enzymes makes such a charge transfer process among DNA-bound $[4Fe4S]^{3+/2+}$ clusters near equilibrium plausible; a dynamic equilibrium between oxidized bound enzymes and reduced dissociated enzymes is expected. As also illustrated in Figure 3.8, the presence of a nearby perturbation in base pair stacking inhibits charge transfer. Under this circumstance, the BER enzyme remains associated with the DNA, allowing DNA-bound facilitated diffusion to the substrate site and repair. This model, then, provides a means to redistribute BER enzymes rapidly away from well matched DNA and preferentially onto genome sites in the vicinity of DNA lesions.

The results given here provide added support for this model. The shift in redox potential for BER enzymes upon DNA binding is now more widely demonstrated. Additionally, since each BER enzyme is in low copy number within the cell, this model provides a means for the enzymes to cooperate in locating their substrates. Some kinetic evidence for cooperativity in enzyme kinetics had been seen previously (*17*), yet there has been no structural evidence for protein dimerization in the bacterial forms of these enzymes. Our model provides for a cooperativity *among* BER enzymes. Indeed, irrespective of the specific substrate for the BER enzyme, none of the enzymes should populate well matched, unperturbed regions of the genome; this model provides a mechanism instead for the enzymes to redistribute onto damaged regions of the genome. Thus, by collaborating in their search for DNA damage, the BER enzymes can efficiently locate their substrates.

Figure 3.8. Proposed model for long range DNA signaling between BER enzymes using DNA-mediated charge transfer to detect base lesions. A collaboration among BER enzymes allows for more efficient sorting onto regions of DNA containing base lesions to facilitate substrate detection by these proteins.

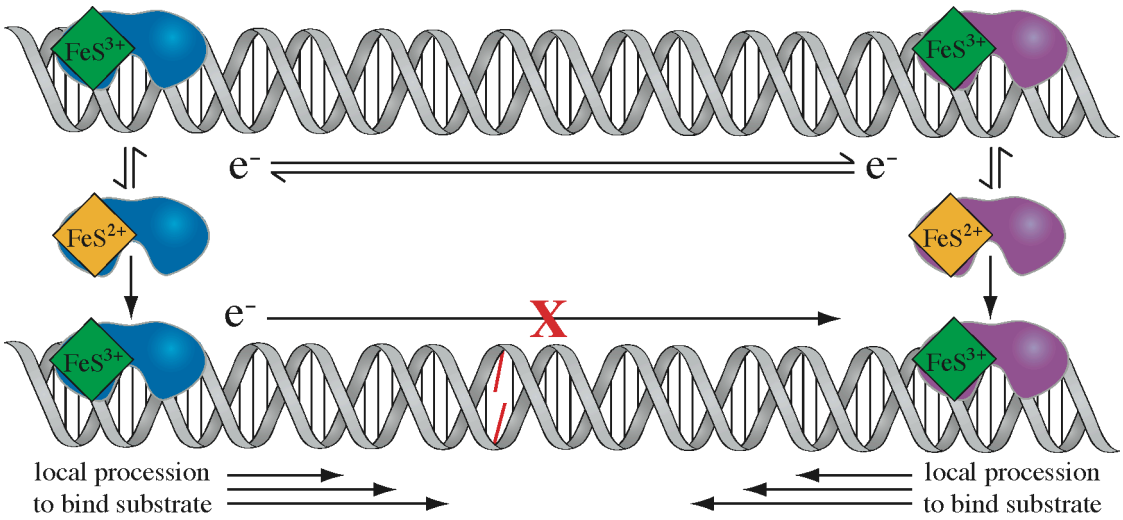

Implications

The [4Fe4S] clusters are ubiquitous in BER enzymes, present in homologues from bacteria to man. A clear functional role for these clusters has been lacking, however. Results here provide a basis for establishing a functional role for the [4Fe4S] clusters of BER enzymes that involves redox chemistry, the common chemistry utilized by most [4Fe4S] cluster-containing proteins within the cell. The role proposed, moreover, involves DNA-mediated charge transfer chemistry, a reaction that has been amply demonstrated to be sensitive to mismatches, lesions, and other perturbations in base pair stacking. Hence these results provide a framework for reconciling the frequency of [4Fe4S] clusters in repair enzymes as well as a strategy for effecting the rapid detection of DNA lesions by repair proteins in low copy number. Significantly, these results also provide a basis for considering how the DNA duplex may provide a medium for long range signaling within the cell.

SUMMARY

MutY and Endonuclease III, two DNA glycosylases from *Escherichia coli*, and AfUDG, a uracil DNA glycosylase from *Archeoglobus fulgidus*, are all base excision repair enzymes that contain the $[4Fe4S]^{2+}$ cofactor. Here we demonstrate that, when bound to DNA, these repair enzymes become redox-active; binding to DNA shifts the redox potential of the $[4Fe4S]^{3+/2+}$ couple to the range characteristic of high potential iron proteins and activates the proteins towards oxidation. Electrochemistry on DNA-modified electrodes reveals potentials for EndoIII and AfUDG of 59 mV and 95 mV versus NHE, respectively, comparable to 90 mV for MutY bound to DNA. In the absence of DNA modification of the electrode, no redox activity can be detected, and on electrodes modified with DNA containing an abasic site, the redox signals are dramatically attenuated; these observations show that the DNA base pair stack mediates electron transfer to the protein and the potentials determined are for the *DNA-bound* protein. In EPR experiments at 10K, redox activation upon DNA binding is also evident to yield the oxidized $[4Fe4S]^{3+}$ cluster and the partially degraded $[3Fe\text{-}4S]^{1+}$ cluster. EPR signals at g= 2.02 and 1.99 for MutY and g= 2.03 and 2.01 for EndoIII are seen upon oxidation of these proteins by $Co(phen)_3^{3+}$ in the presence of DNA and are characteristic of $[3Fe\text{-}4S]^{1+}$ clusters, while oxidation of AfUDG bound to DNA yields EPR signals at g= 2.13, 2.04, and 2.02, indicative of both $[4Fe4S]^{3+}$ and $[3Fe\text{-}4S]^{1+}$ clusters. Based upon this DNA-dependent redox activity, we propose a model for the rapid detection of DNA lesions using DNA-mediated electron transfer among these repair enzymes; redox activation upon DNA binding and charge transfer through well-matched DNA to an alternate bound repair protein can lead to the rapid redistribution of proteins onto genome sites in the vicinity of DNA lesions. This redox activation furthermore

establishes a functional role for the ubiquitous [4Fe4S] clusters in DNA repair enzymes that involves redox chemistry and provides a means to consider DNA-mediated signaling within the cell.

REFERENCES

1. Lindahl, T. (1993) *Nature 362*, 709.

2. Friedberg, E. C., Walker, G. C., and Siede, W. (1995) *DNA Repair and Mutagenesis* ASM Press.

3. Scharer, O.D. (2003) *Angew. Chem. Int. Ed. Engl. 42*, 2946.

4. David, S.S., and Williams, S.D. (1998) *Chem. Rev. 98*, 1221.

5. Verdine, G. L., and Bruner, S. D. (1997) *Chem. Biol. 4*, 329.

6. Stivers, J. T., and Jiang, Y. L. (2003) *Chem. Rev. 103*, 2729.

7. Hamilton, R.W., and Lloyd, R.S. (1989) *J. Biol. Chem. 264*, 17422.

8. Hildebrandt, E. R., and Cozzarelli, N. R. (1995) *Cell 81*, 331.

9. Demple, B., and Harrison, L. (1994) *Annu. Rev. Biochem. 63,* 915.

10. Bregeon, D., Doddridge, Z. A., You, H. J., Weiss, B., and Doetsch, P. W. (2003) *Mol. Cells 12*, 959.

11. Gu, Y., Parker, A., Wilson, T. M., Bai, H., Chang, D. Y., and Lu, A. L. (2002) *J. Biol. Chem. 277*, 11135.

12. Yang, H., Clendenin, W. M., Wong, D., Demple, B., Slupska, M. M., Chiang, J. H., and Miller, J. H. (2001) *Nucleic Acids Res. 29*, 743.

13. Pope, M. A., Porello, S. L., and David, S. S. (2002) *J. Biol. Chem. 277*, 22605.

14. Marenstein, D. R., Ocampo, M. T., Chan, M. K., Altamirano, A., Basu, A. K., Boorstein, R. J., Cunningham, R. P., and Teebor, G. W. (2001) *J. Biol. Chem. 276*, 21242.

15. Marenstein, D. R., Chan, M. K., Altamirano, A., Basu, A. K., Boorstein, R. J., Cunningham, R. P., and Teebor, G. W. (2003) *J. Biol. Chem. 278*, 9005.

16. Liu, X., Choudhury, S., and Roy, R. (2003) *J. Biol. Chem. 278*, 50061.

17. Wong, I., Bernards, A. S., Miller, J. K., and Wirz, J. A. (2003) *J. Biol. Chem. 278*, 2411.

18. Nunez, M. E., Hall, D. B., and Barton, J. K. (1999) *Chem. Biol. 6*, 85.

19. Kelley, S. O., and Barton, J. K. (1999) *Science 283,* 375.

20. Kelley, S. O., Holmlin, R. E., Stemp, E. D. A., and Barton, J. K. (1997) *J. Am. Chem. Soc. 119*, 9861.

21. Holmlin, R. E., Dandliker, P. J., and Barton, J. K. (1997) *Angew. Chem., Int. Edn. Engl. 36*, 2715.

22. Schuster, G. B. (2000) *Acc. Chem. Res. 33*, 253.

23. Giese, B. (2002) *Annu. Rev. Biochem. 71*, 51.

24. Bhattacharya, P. K., and Barton, J. K. (2001) *J. Am. Chem. Soc. 123*, 8649.

25. Hall, D. B., and Barton, J. K. (1997) *J. Am. Chem. Soc. 119*, 5045.

26. Rajski, S. R., and Barton, J. K. (2001) *Biochemistry 40*, 5556.

27. Boon, E. M., Salas, J. E., and Barton, J. K. (2002) *Nat. Biotechnol. 20*, 282.

28. Boon, E. M., Ceres, D. M., Drummond, T. G., Hill, M. G., and Barton, J. K. (2000) *Nat. Biotechnol. 18*, 1096.

29. Nunez, M. E., Noyes, K. T., and Barton, J. K. (2002) *Chem. Biol. 9*, 403.

30. Nunez, M. E., Holmquist, G. P., and Barton, J. K. (2001) *Biochemistry 23*, 12465.

31. Friedman, K. A., and Heller, A. (2001) *J. Phys. Chem. B 105*, 11859.

32. Rajski, S. R., Jackson, B. A., and Barton, J. K. (2000) *Mutat. Res. 447*, 49.

33. Boon, E. M., Livingston, A. L., Chmiel, N. H., David, S. S., and Barton, J. K. (2003) *Proc. Natl. Acad. Sci. U.S.A. 100*, 12543; *ibid. 101*, 4718.

34. Cunningham, R.P., Asahara, H., Bank, J.F., Scholes, C. P., Salerno, J. C., Surerus, K., Munck, E., McCracken, J., Peisach, J., and Emptage, M.H. (1989) *Biochemistry 28*, 4450.

35. Hinks, J.A, Evans, M.C.W., de Miguel, Y., Sartori, A.A., Jiricny, J., and Pearl, L.H. (2002) *J. Biol. Chem. 277*, 16936.

36. Rebeil, R., Sun, Y., Chooback, L., Pedraza-Reyes, M., Kinsland, C., Begley, T. P., and Nicholson, W. L. (1998) *J. Bacteriol. 180*, 4879.

37. Lee, C. H., Kim, S. H., Choi, J. I., Choi, J. Y., Lee, C. E., and Kim, J. (2002) *Mol. Cells 13*, 154.

38. Nghiem, Y., Cabrera, M., Cupples, C. G., and Miller, J. H. (1988) *Proc. Natl. Acad. Sci. U.S.A. 85*, 2709.

39. Michaels, M. L., Cruz, C., Grollman, A. P., and Miller, J. H. (1992) *Proc. Natl. Acad. Sci. U.S.A. 89*, 7022.

40. Michaels, M.L. and Miller, J. H. (1992) *J. Bacteriol. 174*, 6321.

41. Michaels, M. L., Tchou, J., Grollman, A. P., and Miller, J. H. (1992) *Biochemistry 17*, 10964.

42. Gogos, A., Cillo, J., Clarke, N. D., and Lu, A. L. (1996) *Biochemistry 35*, 16665.

43. Lu, A. L., Tsai-Wu, J. J., and Cillo, J. (1995) *J. Biol. Chem. 270*, 23582.

44. Manuel, R. C., Czerwinski, E. W., and Lloyd, R. S. (1996) *J. Biol. Chem. 271*, 16218.

45. Manuel, R. C., and Lloyd, R. S. (1997) *Biochemistry 36*, 11140.

50. Porello, S. L., Leyes, A. E., and David, S. S. (1998) *Biochemistry 37*, 14756.

51. Radicella, J. P., Clark, E. A., and Fox, M. S. (1998) *Proc. Natl. Acad. Sci. U.S.A. 85*, 9674.

52. Guan, Y., Manuel, R. C., Arvai, A. S., Parikh, S. S., Mol, C. D., Miller, J. H., Lloyd, S., and Tainer, J. A. (1998) *Nat. Struct. Biol. 5*, 1058.

53. Michaels, M. L., Pham, L., Nghiem, Y., Cruz, C., and Miller, J. H. (1990) *Nucleic Acids Res. 18*, 3841.

54. Demple, B., and Linn, S. (1980) *Nature 287*, 203.

55. Katcher, H. L., and Wallace, S. S. (1983) *Biochemistry 22*, 4071.

56. Breimer, L. H., and Lindahl, T. (1984) *J. Biol. Chem. 259*, 5543.

57. Duker, N. J., and Weiss, R. B. (1986) *Nucleic Acids Res. 26*, 6621.

58. Boorstein, R. J., Hilbert, T. P., Cadet, J., Cunningham, R. P., and Teebor, G. W. (1989) *Biochemistry 28*, 6164.

59. Wagner, J. R., Blount, B. C., and Weinfeld, M. (1996) *Anal. Biochem. 233*, 76.

60. Dizdaroglu, M., Laval, J., and Boiteux, S. (1993) *Biochemistry 32*, 12105.

61. Kuo, C. F., McRee, D. E., Fisher, C. L., O'Handley, S. F., Cunningham, R. P., and Tainer, J. A. (1992) *Science 258*, 434.

62. Thayer, M. M., Ahern, H., Xing, D., Cunningham, R. P, and Tainer, J. A. (1995) *EMBO J. 14*, 4108.

63. Cowan, J.A., and Lui, S.M. (1998) *Adv. Inorg. Chem. 45*, 313.

64. Fu, W., O'Handley, S., Cunningham, R. P., Johnson, M.K. (1992) *J. Biol. Chem. 267*, 16135.

65. Porello, S. L., Cannon, M. J., and David, S. S. (1998) *Biochemistry 37*, 6465.

66. Lu, A. L., and Fawcett, W. P. (1998) *J. Biol. Chem. 273*, 25098.

67. McGoldrick, J. P., Yeh, Y. C., Solomon, M., Essigmann, J. M., and Lu, A. L. (1995) *Mol. Cell. Biol. 15*, 989.

68. Ikeda, S., Biswas, T., Roy, R., Izumi, T., Boldogh, I., Kurosky, A., Sarker, A. H., Seki, S., Mitra, S. (1998) *J. Biol. Chem. 273*, 21585.

69. Pearl, L.H. (2000) *Mutat. Res.*, *460*, 165.

70. Hoseki, J., Okamoto, A., Masui, R., Shibata, T., Inoue, Y., Yokoyama, S., and Kuramitsu, S. (2003) *J. Mol. Biol. 333*, 515.

71. Knaevlsrud, I., Ruoff, P., Anensen, H., Klungland, A., Bjelland, S., and Birkeland, N. K. (2001) *Mutat. Res. 487*, 173.

72. Sartori, A. A., Schar, P., Fitz-Gibbon, S., Miller, J. H., Jiricny, J. (2001) *J. Biol. Chem. 276*, 29979.

73. Sandigursky, M., Faje, A., and Franklin, W. A. (2001) *Mutat. Res. 485*, 187.

74. Sandigursky, M., and Franklin, W. A. (2000) *J. Biol. Chem. 275*, 19146.

75. Lindahl, T., and Nyberg, B. (1974) *Biochemistry 13*, 3405.

76. Jacobs, K. L., and Grogan, D. W. (1997) *J. Bacteriol. 179*, 3298.

77. Thomas, N.C., Pringle, K., and Deacon, G.B. (1989) *J. Chem. Edu. 66*, 516.

78. Asahara, H., Wistort, P. M., Bank, J. F., Bakerian, R. H., and Cunningham, R. P. (1989) *Biochemistry 28*, 4444.

79. Beaucage, S. L., and Caruthers, M. H. (1981) *Tetrahedron Lett. 22*, 1859.

80. Kelley, S. O.; Boon, E. M.; Barton, J. K.; Jackson, N. M.; Hill, M. G. (1999) *Nucleic Acids Res. 27*, 4830.

81. Tender, L., Carter, M. T., and Murray, R. W. (1994) *Anal. Chem. 66*, 3173.

82. Armstrong, F. A., Heering, H. A., Hirst, J. (1997) *Chem. Soc. Rev. 26*, 169.

83. Guo, L. H., and Hill, H. A. O. (1991) *Adv. Inorg. Chem. 36*, 341.

84. Messick, T. E., Chmiel, N. H., Golinelli, M. P., Langer, M. R., Joshua-Tor, L., and David, S.S. (2002) *Biochemistry 41*, 3931.

85. Camba, R., and Armstrong, F. A. (2000) *Biochemistry 39*, 10587.

86. Roth, E. K. H., and Jordanov, J. (1991) *Inorg. Chem. 30*, 240.

87. Dilg, A. W. E., Mincione, G., Acterhold, K., Iakovleva, O., Mentler, M., Luchinat, C., Bertini, I., and Parak, F. G. (1999) *J. Biol. Inorg. Chem. 4*, 727.

88. Heering, H. A., Bulsink, Y. B. M., Hagen, W. R., and Meyer, T. E. (1995) *Eur. J. Biochem. 232*, 811.

89. Huynh, B. H., Moura, J. J. G., Moura, I., Kent, T. A., Legall, J., Xavier, A. V., and Munck, E. (1980) *J. Biol. Chem. 255*, 3242.

90. Ruzicka, F. J., and Beinert, J. (1978) *J. Biol. Chem. 253*, 2514.

91. Carter, M.T., Rodriguez, M., and Bard, A.J. (1989) *J. Am. Chem. Soc. 111*, 8901.

92. Rehmann, J. P., and Barton, J. K. (1990) *Biochemistry 29*, 1701.

93. Sticht, H., and Rosch, P. (1998) *Prog. Biophys. Mol. Biol. 70*, 95.

94. Fromme, J. C., Banerjee, A., Huang, S. J., and Verdine, G. L (2004) *Nature 427*, 652.

95. Fromme, J. C., and Verdine, G. L (2003) *EMBO J. 22*, 3461.

96. Carter, C.W., Kraut, J., Freer, S.T., Alden, R.A., Sieker, L.C., Adman, E. and Jensen, L.H. (1972) *Proc. Natl. Acad. Sci. USA 69,* 3526.

97. Yavin, E., Boal, A.K., Stemp, E.D.A., Boon, E.M., Livingston, A.L., O'Shea, V.L., David, S.S. and Barton, J.K. (2005) *Proc. Natl. Acad. Sci. USA, 102,* 3546.